Nanomechanical Contribution of Collagen and von Willebrand Factor A in Marine Underwater Adhesion and Its Implication for Collagen Manipulation

Yoo, H. Y., Huang, J., Li, L., Foo, M., Zeng, H. & Hwang, D. S.

Nanomechanical contribution of collagen and von Willebrand factor A in marine underwater adhesion and its implication for collagen manipulation

Hee Young Yoo[a], Jun Huang[b], Lin Li[b], Mathias Foo[c],

Hongbo Zeng[b,] and Dong Soo Hwang[a,d,**]*

[a]Division of Integrative Biosciences and Biotechnology, Pohang University of Science and Technology, Pohang 790-784, Republic of Korea.

[b]Department of Chemical and Materials Engineering, University of Alberta, Edmonton, Alberta T6G 2V4, Canada.

[c]School of Engineering, University of Warwick, Coventry, CV4 7AL, United Kingdom.

[d]School of Environmental Science and Engineering, Pohang University of Science and Technology, Pohang 790-784, Republic of Korea.

ABSTRACT: Recent works on mussel adhesion have identified a load bearing matrix protein (PTMP1) containing von Willebrand factor (vWF) with collagen binding capability that contributes to the mussel holdfast by manipulating mussel collagens. Using Surface Forces Apparatus, we investigate for the first time, the nano-mechanical properties of vWF-collagen interaction using homologous proteins of mussel byssus, PTMP1 and preCollagens (preCols), as collagen. Mimicking conditions similar to mussel byssus secretion (pH < 5.0) and seawater condition (pH 8.0), PTMP1 and preCol interact weakly in the "positioning" phase based on vWF -collagen binding and strengthen in "locked" phase due to the combined effects of electrostatic attraction, metal binding, and mechanical shearing. The progressive enhancement of binding between PTMP1 with porcine collagen under the aforementioned conditions is also observed. The binding mechanisms of PTMP1-preCols provide insights into the molecular interaction of the mammalian collagen system and the development of an artificial extracellular matrix based on collagens.
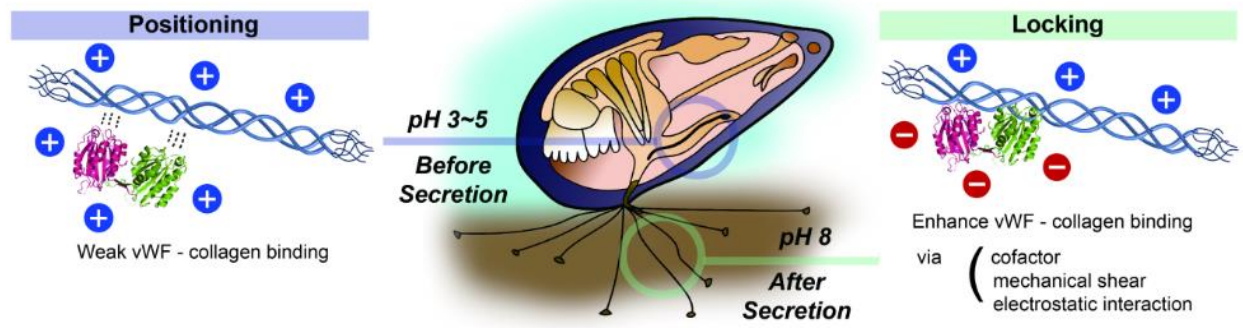
INTRODUCTION

In mammalian tissue, the extracellular matrix (ECM) is composed of a collection of extracellular molecules, which serves as physical support to tissues by residing in the intercellular space.[1-3] Examples of ECM key functions include; benign native scaffolding for cell arrangement within connective tissues, and characterizing cellular behaviors and tissue functions through the use of dynamic, mobile, and flexible components. For the majority of the connective tissues that comprise soft and hard tissues (e.g. bone, cartilage, tendon, blood vessel, skin and so on), the key substance that acts as ECM and forges the organized, three-dimensional (3D) architecture surrounding these cells is the collagen fibrils and its network.[4, 5]

Collagen plays dominant roles in maintaining the biological and structural integrity of the ECM. In line with these key roles, collagen has been widely used as one of the main ECM components in tissue engineering.[6, 7] In particular, engineering 3D scaffolds depends heavily on the ability to manipulate the mechanical properties and morphologies of collagen. Physical or chemical remodeling of the collagen is constantly undergoing adaptation *in vivo* for achieving optimal and proper physiological functions.[4] These can be seen in many examples in mammalian biological systems like the connectivity between bones and skin tissues.[8-10] It is intriguing to note how stiff organs like bones can be inter-connected well with soft organs like skin tissues via connective collagen tissues without incurring severe damages to the latter organs upon the application of load .[11, 12] One possible way for this interaction to be achievable is through the existence of a stiffness gradient between these two organs such that when load is applied to the soft organ, no mechanical mismatch is incurred; more importantly, this stiffness gradient is collagen-mediated.[13, 14] While the formation of this mechanical stiffness gradient comes naturally *in vivo*, to reenact this mechanical stiffness gradient *in vitro* is often not straightforward.[15-17] Furthermore, a lack of

understanding of the physiological collagen manipulation processes has also impeded its practical application to tissue engineering.

Another group of organisms that relies on collagen to function effectively is the marine organism, mussel. Specifically, the mussel byssal threads (byssus) are mostly composed of collagen (> 90 wt%) and these byssal threads act as a holdfast for mussels enabling them to live in their harsh environment. In a similar manner to the efficacy of stiffness gradient of the collagen between bones-skin tissues in mammals, mussel byssus also utilizes this mechanism to overcome the mechanical mismatch between stiff marine substrates and soft mussel tissues. This outstanding load bearing of mussel byssus is partially attributed to the stiffness gradient distribution of two different collagens located at the proximal (preCol-P) and the distal (preCol-D) portions.[18-20] The softer component, preCol-P has a particular motif resembling elastin in the Gly-X-Y tripeptide repeats of the collagens and the harder component, preCol-D has a silk-like motif. What is more interestingly observed in the mussel byssus is the presence of an important protein called Proximal Thread Matrix Protein 1 (PTMP1) that upon interaction with preCol, loosening this collagen structure and subsequently reducing the mechanical mismatch between the hard and soft component in the mussel byssus.[21] PTMP1 is composed of two sequence stretches that are homologous to the group of von Willebrand factor type A3 (vWF-A3) domains whose function is to bind to collagen.[21, 22]

PTMP1 is only found in the proximal region of the byssus making them interact naturally with preCol-P. While this interaction is known, it is only recently that PTMP1 has been shown to induce structural and morphological difference upon its interaction with porcine collagen type I through the vWF A domain and changes the morphology of collagen.[21] Despite this, the understanding of

the nano-mechanical interactions in between vWF A3 and collagen, particularly the adhesion energy under biologically relevant conditions,[23] is still lacking.

In this work, we investigate the nano-mechanical adhesive property of PTMP1 when interacting with preCol and collagen. Using Surface Force Apparatus (SFA), the adhesion strengths of not only PTMP1 and preCol but also type I vertebrate collagen are measured for the first time. Our results show that PTMP1 interacts strongly with preCol and collagen under varying conditions and this provides invaluable insights into the mechanistic role of this crosslinker in its interaction with collagen, which would subsequently be useful for tissue engineering. Our findings suggest that the marine adhesion system should be fully explored with important implications in the advancement of tissue engineering.

MATERIALS AND METHODS

PreCol Purification from Mussel Feet. Mussels (*Mytilus californianus*) were harvested from Goleta Pier (Goleta, CA) and maintained in mariculture at 12 to 15 °C. Whole feet were dissected from mussels and frozen on glass plates at –80 °C. preCols were purified from frozen *M. californianus* feet according to published procedures.[24] Sample purity was assessed using acid urea polyacrylamide gel electrophoresis, amino acid analysis, and MALDI-TOF mass spectrometry.

PTMP1 Purification. A cDNA of PTMP1 was designed and synthesized based on *E. coli* K12 codon usage preference. To express PTMP1 in *E. coli*, the cDNA of PTMP1 with the major codons of *E.coli* was cloned into pET28b(+) with Nco I and Hind III enzyme sites, and transformed into *E. coli* BL21(DE3). Cultures were performed in 2xTY medium supplemented with 50 μg/ml Kanamycine (Sigma, St. Louis, USA) as a selection marker at 37 °C and 250 rpm. Cell growth was monitored by optical density at 600 nm (OD600) using an ultraviolet (UV)–visible

spectrophotometer (OPTIZEN POP, Mecasys, Daejeon, S. Korea). When the cultures reached 0.2 $\leq OD_{600} \leq 0.5$, 1 mM (final concentration) isopropyl-b-D-thiogalactopyranoside (IPTG) was added to culture broth to induce PTMP1 production. The samples were harvested 9 h after the induction, then centrifuged at 18,000 x g for 10 mins at 4 °C; the cell pellets were resuspended in 5 ml lysis buffer (10 mM Tris-Cl, 100 mM sodium phosphate, pH 8.0) per gram wet weight. Samples were lysed by constant cell disruption systems (Constant Systems) at 20 KPSI and lysates were centrifuged at 18,000 x g for 20 mins at 4 °C and the cell debris was collected for purification. The cell lysate pellet was resuspended in 5% (v/v) acetic acid to extract PTMP1. The extracting solution was centrifuged at 18,000 x g for 20 mins at 4 °C and the supernatant was collected and dialyzed in 5% (v/v) acetic acid buffer overnight at 4 °C using Spectra/Por molecular porous membrane tubing (MWCO 1,000 Da, Spectrum Laboratories, USA). Then the purified sample was concentrated by freeze-drying for further purification. The concentrated PTMP1 was injected into an Aquapore RP-300 column (C8, 250 X 7.0 mm, Brownlee, Perkin-Elmer, USA) with a flow rate of 1.0 ml/min with the same gradient condition used in previous method for mfp-1 purification. The purity of PTMP1 (~95%) was confirmed by SDS-PAGE and amino acid analysis.

Force vs. Distance Profiles Measured by an SFA. An SFA system (SurForce LLC, Santa Barbara, CA, USA) was used to measure the interaction forces of protein films in different aqueous solutions. Detailed setup of the SFA system and its working principles can be found in.[25] Briefly, two back-silvered thin mica surfaces with thickness ~1 to 5 μm were glued onto cylindrical silica disks that had a curvature radius R ~2 cm. For PTMP1 vs. mica experiments, only one mica surface was coated with PTMP1 protein layer. For PTMP1 vs. collagen experiments, both mica surfaces were coated with PTMP1 protein-layer at pH 3.0, then one of the PTMP1 coated surfaces was drop coated with collagen solution for 20 mins.[26]

In both cases, the two disks were mounted in the SFA system in a cross-cylinder configuration, the interaction of which is equivalent to that of a sphere with radius R approaching a flat surface when the separation distance $D \ll R$. Desired buffer solutions were injected between the two surfaces for further force measurement.

The interaction forces of protein functionalized mica surfaces were measured in Acetic acid solution with pH 3.0, or in PBS buffer with pH 5.0 or 8.0. The film thickness and separation distance can be obtained *in situ* by using an optical technique called Multiple Beam Interferometry (MBI) using Fringe of Equal Chromatic Order (FECO). Based on the Derjaguin approximation, the measured force $F(D)$ between two curved surfaces separated by D can be correlated to the interaction energy per unit area $W(D)$ of two flat surfaces separated by D:

$F(D) = 2\pi R W(D)$

For the shear experiment, the piezo bimorph of the SFA was operated at a frequency of 0.005 Hz with sliding distance of 1 μm, and the two surfaces were kept sliding for 3 cycles before normal force measurement.

Atomic Force Microscopy (AFM). PTMP1-coated surfaces were inspected in air using AFM in tapping mode (Nanoscope III, Digital Instrument, Santa Barbara, CA, USA). Before imaging, three droplets of PTMP1 solution (pH 3.0) in the presence and the absence of 10 μM preCols or collagens, were placed on a freshly-cleaved mica surface for about 20 mins, then rinsed several times with buffer solution to remove excess proteins and with pure Milli-Q water to remove salt, then air dried in a laminar-flow hood.

Transmission Electron Microscopy (TEM). A mussel proximal foot was covered with the flat side of another B-type planchette and rapidly frozen in a Bal-Tec HPM 010 high-pressure freezer (Boeckeler Instruments). After freeze substitution for 5 days at −80 °C in anhydrous acetone

containing 2% OsO4, the samples were warmed to room temperature over 2 d (24 h from −80 °C to −20 °C , 20 h from −20 °C to 4 °C , 4 h from 4 °C to 20 °C). The samples were washed three times with anhydrous acetone, then embedded in a graduated Epon resin (Ted Pella Inc.) dilution in acetone (5, 15, 25, 50, 75 and 100%) over 3 d. The samples were polymerized at 60 °C in an oven for 24 h, then sectioned and post-stained with aqueous 2% uranyl acetate and Reynolds lead citrate solution.

RESULTS

Interaction between PTMP1 and Mica at Different pH. Recombinant PTMP1 was produced and purified from *E. coli* (Fig. 1A). PreCols were purified from the feet of mussels (*Mytilus californianus*) (Fig. 1B). The interaction force between mica and a PTMP1 layer coated on mica (asymmetric configuration) was measured using an SFA at three pH values. The two surfaces were first brought together to reach a so-called hard (steric) wall distance D_{hw}, then separated. Here, D_{hw} is defined as the separation distance between two surfaces that remains almost unchanged when the normal compressive load or pressure are increased; i.e., D_{hw} measures the thickness of the proteins that are confined between two surfaces. In this asymmetric configuration, the measured D_{hw} of a PTMP1 coating on mica was ~6 nm, which is the same as the diameter of PTMP1 as resolved by X-Ray crystallography (~6 nm).[21] This result proves that the mica was coated with a roughly monomolecular layer of PTMP1.

The formation of mussel byssal thread depends critically on pH; the proteins are secreted at pH 2.2–3.3, then hover transiently at pH 4.0–6.0 before equilibrating with seawater ~pH 8.2.[24] Therefore, to simulate the pH condition for PTMP1 adhesion before and after secretion, the experiments were conducted at pH = 3.0, 5.5, and 8.0.

From the normalized force-distance (F/R vs. D) curve (Fig. 2A), the adhesion between PTMP1 and mica was $W_{ad} \approx -0.5 \pm 0.005$ mJ/m^2 at pH 3.0. The charge of the amino acid in the proteins can vary depending on the solution pH and the isoelectric point (pI) of the protein. PTMP1 has pI ~5.9.[21] At pH < pI, protonation of amino acid residues in PTMP1 increases its positive charge, thereby strengthening its electrostatic attraction to the negatively-charged mica surface. Increasing the buffer pH from 3.0 to 5.5 resulted in the decreased of the adhesion strength between PTMP1 and mica to $W_{ad} \approx -0.2 \pm 0.010$ mJ/m^2. This result is mainly because the positive charge on PTMP1 decreases as pH increases from 3.0 to 5.5, as the electrostatic attraction between PTMP1 and mica decreases. At pH 8.0, PTMP1 becomes negatively charged, so it does not adhere to mica. The decreased adhesion with increasing pH measured above implies that the attraction between PTMP1 and mica could be weakened due to the increased electrostatic repulsion at high pH condition.

Interaction between PTMP1 Surfaces at Different pH. The interactions between two PTMP1 layers (symmetric configuration) were also measured using the SFA at pH 3.0, 5.5 and 8.0. In this symmetric configuration D_{hw} increased to ~12 nm from 6 nm; indicating that both mica surfaces are coated with a monomolecular layer of PTMP1. Varying the pH of the solution did not substantially affect the interaction between the two PTMP1 films (Fig. 2B); therefore PTMP1 surfaces do not adhere to each other at $3.0 \leq pH \leq 8.0$.

Interaction between PTMP1 and preCol at Different pH. The collagen-like domain in preCols may interact with the vWF domain of PTMP1 in the mussel byssal thread; therefore preCols were purified from the mussel feet and used for direct force measurements with PTMP1. For SFA measurement of the interaction between PTMP1 and preCols, PTMP1 was first coated on both mica surfaces, then preCols purified from mussel (Fig. 1B) were deposited on one of the

two PTMP1 surfaces. The mica coated with preCols was rinsed thoroughly with 0.1M acetic acid solution to remove excess protein. At the end of each rinse, a large drop of selected buffer solution (i.e. pH 3,0, 5.5, and 8.0) was left on the coated surface to ensure that it stayed wet before being mounted in the SFA chamber. Successful deposition of preCols on PTMP1 was confirmed by AFM imaging (Fig. S1). The adhesion measured between PTMP1 and preCols increased from W_{ad} ≈ –0.2 ±0.006 at pH 3 to W_{ad} ≈ –0.9 ± 0.008 mJ/m^2 at pH 8.0 (Fig. 2C).

Effect of Contact Time. The contact time was fixed at 1 min in the aforementioned force measurements, and an adhesion energy W_{ad} ≈ –0.9 ± 0.008 mJ/m^2 was measured between PTMP1 and preCols (Fig. 2C). As the contact time increased to 30 mins, the adhesion increased to W_{ad} ≈ –2.8 ± 0.024 mJ/m^2 (Fig. 3B). The interaction between PTMP1 and preCols appears to show strong adhesion that reaches ~60% of the "gold standard" of noncovalent protein-ligand binding i.e., avidin–biotin[27] and 90% of the interaction of DOPA in mussel foot protein-1 with tris- and bis-catecholate complexes with Fe^{3+}.[28]

The enhanced adhesion with increasing contact time is presumably mainly due to the conformational rearrangement of the protein chains to increase the number of exposed binding sites on both PTMP1 and preCols at the contact interface. Successive re-approach and separation between PTMP1 and PTMP1 coated with preCols (contact time ~1 min) was conducted immediately following the measurement with 30 mins contact time; the force-distance profile shows similar adhesion (i.e. W_{ad} ≈ –2.8 ± 0.024 mJ/m^2). This result suggests that once the conformation re-arrangement occurs at the PTMP1-preCols interface, it does not return to its original state immediately.

Effect of cofactor Zn^{2+}. PTMP1 has two domains that are homologous to the group of vWFA-3A domains. In the vWFA-3A domain, the metal ion coordinating motif (DXSXSyTyD) is the part

to which only Zn^{2+} can bind. This particular motif is also known as the metal ion adhesion sites (MIDAS)[29, 30] and this sequence motif is found in one of the vWFA domains (A1 domain) of PTMP1. As a note, the cofactor for the vWF3 domain in PTMP1 is Zn^{2+}, while the cofactor that is involved in collagen and the vWF domain is Ca^{2+}.

As PTMP1 has a MIDAS motif, force measurements were conducted to investigate the effect of Zn^{2+} on adhesion between PTMP1 and preCols at pH 8.0. For interactions between the PTMP1 and preCols (with 1 min contact time), the addition of ~10 μM Zn^{2+} enhanced the adhesion ($W_{ad} \approx -3.6 \pm 0.351$ mJ/m^2) as compared to the case without Zn^{2+} ($W_{ad} \approx -0.9 \pm 0.008$ mJ/m^2) (Fig. 3B). Increasing the contact time from 1 min to 30 min did not substantially increase the adhesion ($W_{ad} \approx -3.9 \pm 0.162$ mJ/m^2).

The presence of Zn^{2+} increased the adhesion between of PTMP1 and preCol by a factor of four. It is speculated that at the ion-binding pocket provided by the MIDAS motif, the presence of metal ions enhanced the binding of preCol to PTMP1.

Effect of Shear. The proximal thread shows strain-stiffening behavior when subjected to repetitive loading.[31] This behavior suggests that binding between PTMP1 and preCols could be enhanced under shear condition. To test this hypothesis, the interaction force between PTMP1 and preCols under shear condition was measured.

A mica surface coated with PTMP1 was brought into contact with a mica surface on which preCols were coated onto PTMP1, sheared laterally at 10 nm/s with shearing amplitude of 1 μm for three cycles. The shearing was then stopped, and the surfaces were kept in contact for 1 min. The measured adhesion was $W_{ad} \approx -4.3 \pm 0.013$ mJ/m^2 (Fig. 4A). As the contact time was increased to 30 mins, the adhesion increased to $W_{ad} \approx -5.3 \pm 0.022$ mJ/m^2. Similar experiments were conducted at shear rate ≥ 200 nm/s, and we observed preCols has a tendency to form aggregates

with PTMP1 (Figs. S2A, B). Under this condition, preCols became tangled to form a thick fibril assembly (Fig. S2B). This process eventually led to the increase of D_{hw}: the smooth flat contact region before shearing (Fig. S2C) deformed due to the presence of the confined aggregates formed during shearing (Fig. S2D). Under shear conditions, the stiffness of protein assemblies of vWF domains interacting with collagens increases.[32] Because PTMP1 has vWFA domains, the "stiffening" (i.e., enhanced adhesion) of PTMP1 and preCol may result from enhanced interaction and entanglement between PTMP1 and preCol induced by shearing. This finding is in agreement with the observation that continued cyclic loading of the byssal thread increases its stiffness.[31]

Interaction of PTMP1 and type I Vertebrate Collagen. All the above results on the interactions between PTMP1 and preCol emphasize that PTMP1 and preCol possess vWF A3-like and collagen-like properties, respectively. Given that the vWF A3-collagen interaction is crucial for ECM environment, the interaction of a vWF A3 like PTMP1 with collagen could provide insights into this adhesion.

Therefore, we considered PTMP1 and porcine type-I collagen, and repeated the experiments involving the effect of contact time, addition of cofactor Zn^{2+} and shearing on the interaction between these proteins. Porcine type-I collagen is a structurally well-defined collagen that forms largely parallel arrays of collagen fibrils[33] *in vivo*. The homogenous and planar topography of the collagen matrices guarantee that any differences in adhesion are related to protein-specificity and not due to the topography of the matrices.

The measured adhesion force between PTMP1 and collagen was $W_{ad} \approx -0.2 \pm 0.010$ mJ/m^2 at pH 8.0 (Fig. 3C). This adhesion strength is weaker as compared to that of PTMP1-preCol (Fig. 3B); thus the decrease is expected given that preCol is the natural binding substance to PTMP1. Nonetheless, the results are encouraging because they show that although collagen is not the

natural substance to which PTMP1 binds, weak adhesion still occurs, possibly due to the presence of the vWF A3 component in PTMP1. Additionally, this result also indicates that the collagen domain in preCol is most likely the major domain that is responsible for the adhesion measured above as the mediator of the adhesion is through its vWF A3 domain. Nevertheless, it is noted that given that the flanking and histidine rich domains made up almost 50% of the amino acid sequence of preCol, these domains could also potentially contribute to the interaction.[24]

The effect of contact time between PTMP1 and collagen showed a similar (although weaker) trend to the one observed for PTMP1 and preCol (Fig. 3B). The increase in adhesion with contact time in PTMP1-collagen is due to possible adaptation of PTMP1 to have ligand substrate binding with collagen.

The effect of Zn^{2+} on the interaction between PTMP1 and collagen was investigated. Again, the response was similar to, although weaker than, the interaction between PTMP1 and preCol. The addition of Zn^{2+} increased the adhesion from $W_{ad} \approx -0.2 \pm 0.010$ mJ/m^2 to $W_{ad} \approx -0.8 \pm 0.002$ mJ/m^2 after 1 min contact time (Fig. 3C). We speculate that the increase in adhesion was due to collagen positioning along the negative charges of the vWFA domain of PTMP1. Because PTMP1 has a MIDAS motif, the addition of Zn^{2+} may enhance a specific adhesion between collagen and PTMP1. It is noted that Zn^{2+} can facilitate the binding on the flanking and histidine domains [34, 35] but it would not be a major contributor for the attraction because of the steric hindrance between two domains. On the other hand, as porcine collagen is not the natural binding substance of PTMP1, and there is no flanking and histidine domain, the addition of Zn^{2+} does lead to the formation of the incomplete Zn^{2+} coordination complexes, thus yielding a weaker adhesion.

It has been reported that shear can also cause binding of collagens to the vWFA domain.[36-38] Hence, to test the idea that adhesion can be enhanced by shear between vWF A3 and collagen

because of the presence of vWF A3 domain, we measured the interaction between PTMP1 and collagen subjected to the same shearing condition used in the test of PTMP1 and preCol. Application of shearing increased the adhesion from $W_{ad} \approx -1.2 \pm 0.008$ mJ/m^2 to $W_{ad} \approx -2.5 \pm 0.006$ mJ/m^2 (Fig. 4B). This finding is in agreement with a previous report that shear stress events strengthen the adhesion of collagen to vWF.[39]

The PTMP1-collagen interactions over three different effects were qualitatively similar to, although consistently weaker than, results obtained for PTMP1-preCol. These results are encouraging because they provide a useful clue to the mechanism of interaction between vWF 3A and collagen in ECM.

DISCUSSIONS

Underwater adhesion by the mussel byssus involves an interaction between preCol and PTMP1, which are similar to mammalian collagen and the vWF A3 domain. We exploited these similarities and used the understanding of the mechanism of underwater adhesion of mussel byssus threads to gain insights into the mechanism behind the molecular interactions of the mammalian collagen system.

The formation of mussel byssus from preCols and PTMP1 occurs over a range of pH 3.0–5.0 during secretion from the mussel foot to pH ~8.0 under seawater condition outside the foot.[40] Subsequent muscular contractions that induce mechanical shear stresses between mussel foot and immature byssus are conducted for ~3 mins to fix the byssus structure. Therefore, factors that influence the adhesion such as effects of pH, normal stress, metal binding, and shearing were investigated (Fig. 5).

The SFA measurements between PTMP1 and preCols under different pH conditions reveal that the adhesion energy is highly pH-dependent, mainly as a result of the effects of pH on electrostatic interactions and the isoelectric points of the proteins (Fig. S3). Before secretion of the mixture of collagen, the proteins are stored in acidic medium at $3.0 \leq pH \leq 5.0$, where both of them are positively charged. The positively-charged PTMP1 (pI ~5.9) and preCol-P[41] (pI ~10) interact and form a complex by overcoming long-range electrostatic repulsion at pH 3.0 (Fig. 2C, red). Cryo-TEM results of mussel secretory granules also indicate that PTMP1 and preCol-P can interact and form complexes (Fig. S4). However, the binding between PTMP1 and preCol-P remains dynamic until they are secreted and reach equilibration with seawater. When the mixture of preCol-P is released to seawater (pH ~8.2) to form a byssal thread (collagenous fiber), a drastic charge inversion of PTMP1 (pKa ~5.9) from positive to negative occurs and increases the strength of the binding (locking) to the positively-charged preCol-P at pH 8.0 (Fig 1C, purple curve).

Zn^{2+} ion is a cofactor for the adhesion, and is most effective at pH 8.0. PTMP1 contains a MIDAS motif,[21] which provides a pocket to facilitate the binding Zn^{2+}. As the presence of Zn^{2+} may mediate bridging attraction between negatively charged PTMP1 films via metal coordination, the effect of Zn^{2+} on the interaction between two layers of PTMP1 was measured and no substantial adhesion was observed with the addition of Zn^{2+} (as shown in Fig. S5). Increase in adhesion after introduction of metal ions has also been observed in vWF A3 and collagen.[42]

The mechanical normal and shear stresses given by the muscular contractions of the mussel foot induce conformational rearrangement of the interface between PTMP1 and preCol-P; on the protein chains this rearrangement increases the number of binding sites that are exposed at the interface during mechanical contact and this induced fit leads to increased binding strength (Figs. 2, 3). Shearing also alters adhesion in the vWF domain and in collagen. The effect of shearing on

the strengthening of adhesion was tested using SFA and our results support this mechanism. The effect of shearing is more prominent in proteins that have a vWF domain that interacts with collagen[37, 38] than in proteins that do not have this domain and this observation corresponds to the interaction between PTMP1 and preCol under shearing. High shear rate led to aggregation or entanglement of PTMP1 and preCol (Fig. S2B), thereby impeding measurement of adhesion. Nevertheless, this situation would not affect mussels in nature because this entanglement is a reversible process, which is not possible *in vitro*.

Mechanical locking between the collagen and the matrix is finally achieved by a combination of pH, metal (cofactor) binding, and shear stress triggers to enhance interaction. The ultimate interaction energy between PTMP1 and preCols after secretion is comparable to the biotin-avidin ligand binding interaction, and is fully reversible.[27]

What implications can we draw from our findings? A recent biochemical study indicated that the vWF domain is present in the adhesive protein of marine fouling organisms and also in collagen based materials in vertebrates.[32] Our results using SFA measurements has revealed that the interaction of collagen with the vWF domain results in increased adhesion in the presence of mechanical shear and cofactor metal ion and that these phenomena increase the adhesive strength of marine fouling organisms. This mechanism is very similar to the adhesion mechanism of collagens and platelets, because vWF adhesion shows pH dependency and locking[43, 44] under mechanical shear, and involves cofactor binding with Ca^{2+}.[36, 42, 45, 46] Therefore, the results from this work could provide insights into the development of ECM systems that involve the vWF domain and collagen, and that work in saline conditions.

For practical applications, factors (i.e. shearing and metal ions) that affect this binding adhesion must be considered when evaluating tissue engineering applications with regard to collagen. For

example, in tissue-engineering scaffolds, this binding-adhesion approach can be applied to 3D bioprinting technology that uses vWF and collagen; i.e., the mechanical properties of the vWF and collagen mixture can be controlled by applying shear stress, by changing pH, or by supplying cofactors.

CONCLUSIONS

Our results indicate that the adhesion between PTMP1 and preCol through the vWF domain is strong in seawater, pH dependent, reversible, increased as shear was applied, and increased with addition of metal cofactor. All of these characteristic can be applicable to the biomaterials design process based on vWF and collagen. Overall, the binding mechanisms between PTMP1-preCols provide insights into the molecular interaction of the mammalian collagen system and the development of artificial extracellular matrix based on collagens.

SUPPORTING INFORMATION

AFM tapping mode images (Figure S1), TEM and FECO views of the adhesion experiment (Figure S2), Isoelectric point curve of PTMP1 and preCol-P (Figure S3) and Cryo-TEM image of PTMP1 antibody that binds to the mussel preCol-P (Figure S4), SFA measurements of symmetrical PTMP1 with addition of Zn^{2+} (Figure S5) (PDF).

AUTHOR INFORMATION

*Corresponding author.

Email: hongbo.zeng@ualberta.ca (H.Z.)

**Corresponding author.

Email: dshwang@postech.ac.kr (D.S.H)

Author Contributions.

H.Y.Y. and J.H. contributed equally. H.Z. and D.S.H. conceived the project and the experimental design. H.Y.Y., J.H., M.F., and L. L. performed and analysed the experiments. H.Y.Y., J.H., M.F., H.Z., and D.S.H. wrote the paper.

Notes:

The authors declare no conflict of interest.

ABBREVIATIONS

PTMP1, Proximal Thread Matrix Protein-1; preCol-P, preCollagen-Proximal; preCol-D, preCollagen-Distal; vWF, von Willebrand Factor; SFA, Surface Force Apparatus; AFM, Atomic Force Microscopy; TEM, Transmission Electron Microscopy, MBI, Multiple Beam Interferometry; FECO, Fringe of Equal Chromatic Order.

ACKNOWLEDGEMENTS

and for critical reviews and comments. We also thank Felicity Kendrick and Iulia Gherman for their critical comments.

REFERENCES

(1)   Chan, B. P.; Leong, K. W. (2008) *Eur. Spine J. 17*, 467-479.

(2)   Ye, Z.; Mahato, R. I. (2008) *Nanomedicine 3*, 5-8.

(3)   Farach-Carson, M.; Wagner, R.; Kiick, K. (2007) *Extracellular matrix: structure, function, and applications to tissue engineering*. CRC Press: Boca Raton, FL, USA: pp 3-1.

(4)   Cen, L.; Liu, W.; Cui, L.; Zhang, W.; Cao, Y. (2008) *Pediatr. Res. 63*, 492-496.

(5)   Murasawa, Y.; Hayashi, T.; Wang, P.-C. (2008) *Exp. Cell Res. 314*, 3638-3653.

(6)   Chu, P. K.; Liu, X. (2008) *Biomaterials fabrication and processing handbook*. CRC press.

(7)   Burdick, J. A.; Mauck, R. L. (2010) *Biomaterials for tissue engineering applications: a review of the past and future trends*. Springer Science & Business Media.

(8)   Buehler, M. J.; Ackbarow, T. (2007) *Mater. Today 10*, 46-58.

(9)   Taylor, D. (2007) *J. Mater. Sci. 42*, 8911-8918.

(10)   Ferreira, A. M.; Gentile, P.; Chiono, V.; Ciardelli, G. (2012) *Acta Biomater. 8*, 3191-3200.

(11)   Pal, S. (2014) *Design of Artificial Human Joints & Organs*. Springer.

(12)   Haut, R., Biomechanics of Soft Tissue. In *Accidental Injury*, Nahum, A.; Melvin, J., Eds. Springer New York: 2002; pp 228-253.

(13)   Stahl, P. J.; Romano, N. H.; Wirtz, D.; Yu, S. M. (2010) *Biomacromolecules 11*, 2336-2344.

(14)   Sundararaghavan, H. G.; Monteiro, G. A.; Firestein, B. L.; Shreiber, D. I. (2009) *Biotechnol. Bioeng. 102*, 632-643.

(15)   Sant, S.; Hancock, M. J.; Donnelly, J. P.; Iyer, D.; Khademhosseini, A. (2010) *Can. J. Chem. Eng. 88*, 899-911.

(16)   Gattazzo, F.; Urciuolo, A.; Bonaldo, P. (2014) *Biochim. Biophys. Acta 1840*, 2506-2519.

(17)   Tse, J. R.; Engler, A. J. (2011) *PLoS ONE 6*, e15978.

(18)   Waite, J. H.; Lichtenegger, H. C.; Stucky, G. D.; Hansma, P. (2004) *Biochem. 43*, 7653-7662.

(19)   Coyne, K. J.; Qin, X.-X.; Waite, J. H. (1997) *Science 277*, 1830-1832.

(20)   Waite, J. H.; Andersen, N. H.; Jewhurst, S.; Sun, C. (2005) *J. Adhesion 81*, 297-317.

(21)   Suhre, M. H.; Gertz, M.; Steegborn, C.; Scheibel, T. (2014) *Nat. Commun. 5*.

(22)   Suhre, M. H.; Scheibel, T.; Steegborn, C.; Gertz, M. (2014) *Acta Crystallogr. F-Struct. Biol. Cryst. Commun. 70*, 769-772.

(23)   Friedrichs, J.; Helenius, J.; Muller, D. J. (2010) *Nat. Protoc. 5*, 1353-1361.

(24)   Harrington, M. J.; Waite, J. H. (2007) *J. Exp. Biol. 210*, 4307-4318.

(25)   Israelachvili, J.; Min, Y.; Akbulut, M.; Alig, A.; Carver, G.; Greene, W.; Kristiansen, K.; Meyer, E.; Pesika, N.; Rosenberg, K.; Zeng, H. (2010) *Rep. Prog. Phys. 73*, 036601.

(26)   Martinez Rodriguez, N. R.; Das, S.; Kaufman, Y.; Wei, W.; Israelachvili, J. N.; Waite, J. H. (2015) *Biomaterials 51*, 51-57.

(27)   Helm, C. A.; Knoll, W.; Israelachvili, J. N. (1991) *Proc. Natl. Acad. Sci. U.S.A. 88*, 8169-8173.

(28)   Zeng, H.; Hwang, D. S.; Israelachvili, J. N.; Waite, J. H. (2010) *Proc. Natl. Acad. Sci. U.S.A. 107*, 12850-12853.

(29)   Jokinen, J.; Dadu, E.; Nykvist, P.; Käpylä, J.; White, D. J.; Ivaska, J.; Vehviläinen, P.; Reunanen, H.; Larjava, H.; Häkkinen, L.; Heino, J. (2004) *J. Biol. Chem. 279*, 31956-31963.

(30)   Lee, J.-O.; Rieu, P.; Arnaout, M. A.; Liddington, R. (1995) *Cell 80*, 631-638.

(31)   Sun, C.; Vaccaro, E.; Waite, J. H. (2001) *Biophys. J. 81*, 3590-3595.

(32)   Sun, C.; Lucas, J. M.; Waite, J. H. (2002) *Biomacromolecules 3*, 1240-1248.

(33)   Orgel, J. P. R. O.; Miller, A.; Irving, T. C.; Fischetti, R. F.; Hammersley, A. P.; Wess, T. J. (2001) *Structure 9*, 1061-1069.

(34)   Schmitt, C. N. Z.; Politi, Y.; Reinecke, A.; Harrington, M. J. (2015) *Biomacromolecules 16*, 2852-2861.

(35)   Schmidt, S.; Reinecke, A.; Wojcik, F.; Pussak, D.; Hartmann, L.; Harrington, M. J. (2014) *Biomacromolecules 15*, 1644-1652.

(36)   Cruz, M. A.; Yuan, H.; Lee, J. R.; Wise, R. J.; Handin, R. I. (1995) *J. Biol. Chem. 270*, 10822-10827.

(37)   Schneider, S. W.; Nuschele, S.; Wixforth, A.; Gorzelanny, C.; Alexander-Katz, A.; Netz, R. R.; Schneider, M. F. (2007) *Proc. Natl. Acad. Sci. U.S.A. 104*, 7899-7903.

(38)   Novák, L.; Deckmyn, H.; Damjanovich, S.; Hársfalvi, J. (2002) *Blood 99*, 2070-2076.

(39)   Emsley, J.; Knight, C. G.; Farndale, R. W.; Barnes, M. J.; Liddington, R. C. (2000) *Cell 101*, 47-56.

(40)   Lee, B. P.; Messersmith, P. B.; Israelachvili, J. N.; Waite, J. H. (2011) *Annu. Rev. Mater. Res. 41*, 99-132.

(41)   Harrington, M. J.; Waite, J. H. (2008) *Biomacromolecules 9*, 1480-1486.

(42)   LaDuca, F.; Bettigole, R.; Bell, W.; Robson, E. (1986) *Blood 68*, 927-937.

(43)   Jagielska, A.; Wilhite, K. D.; Van Vliet, K. J. (2013) *PLoS ONE 8*, e76048.

(44)   Paradise, R. K.; Whitfield, M. J.; Lauffenburger, D. A.; Van Vliet, K. J. (2013) *Exp. Cell Res. 319*, 487-497.

(45)   Coller, B. S. (1978) *J. Clin. Invest. 61*, 1168-1175.

(46)   Shim, K.; Anderson, P. J.; Tuley, E. A.; Wiswall, E.; Evan Sadler, J. (2008) *Blood 111*, 651-657.
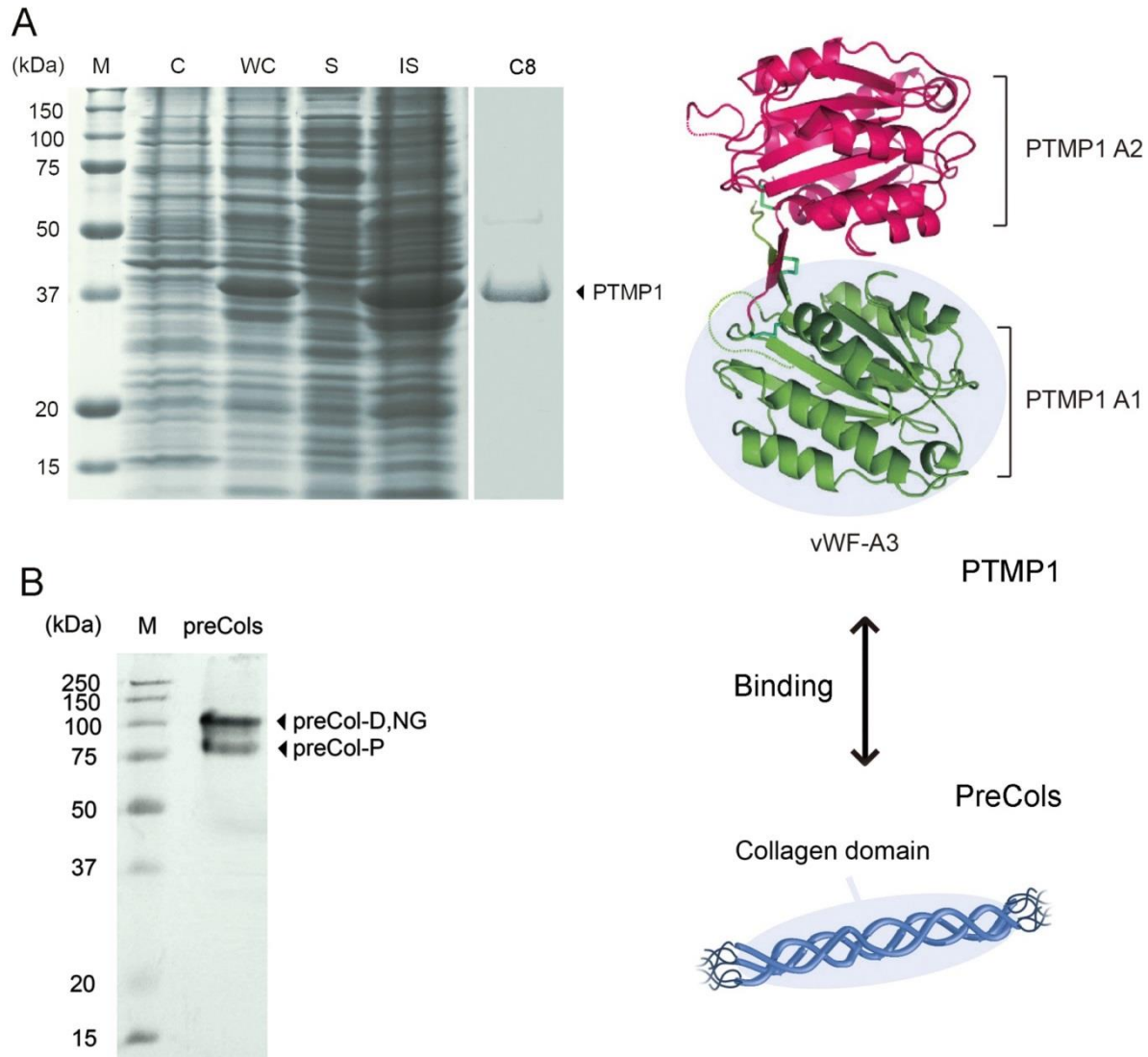
TABLES OF CONTENT GRAPHICS

Figure 1. (A) SDS-PAGE with Coomasie blue staining and 15% gels were used for PTMP1 purification. Lanes: M, protein molecular weight marker; C, whole-cell sample containing the parent vector pET28b+ (negative control); WC, whole-cell sample; S, soluble supernatant fraction; IS, insoluble cell debris fraction; C8, used HPLC C8 column for separation of PTMP1. (B) SDS-PAGE with Coomasie blue staining and 15% gels were used for Precols purification. Lanes: M, protein molecular weight marker; preCols: extracted purified preCols.
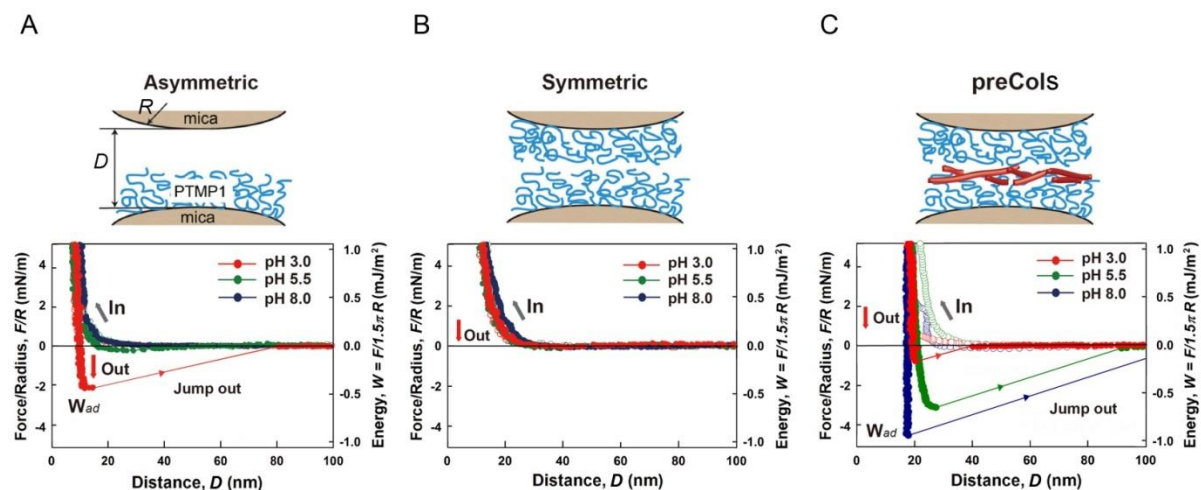
Figure 2. SFA studies of PTMP1 adhesion on mica (asymmetric configuration) and cohesion (symmetric configuration) in standard buffer solution pH 3.0, 5.5, 8.0. (A) PTMP1 vs. mica; (B) PTMP1 vs. PTMP1. (C) PTMP1 vs. PreCols. The normalized forces, F/R is denoted in the left ordinate, whereas the corresponding interaction energies per unit area, W (defined by $W = F/1.5\pi R$) is on the right ordinate. W_{ad} is the adhesion energy per unit area ($W_{ad} = F_{ad}/1.5\pi R$). Open circle shows "in" (approach) and filled circle is "out" (separation).
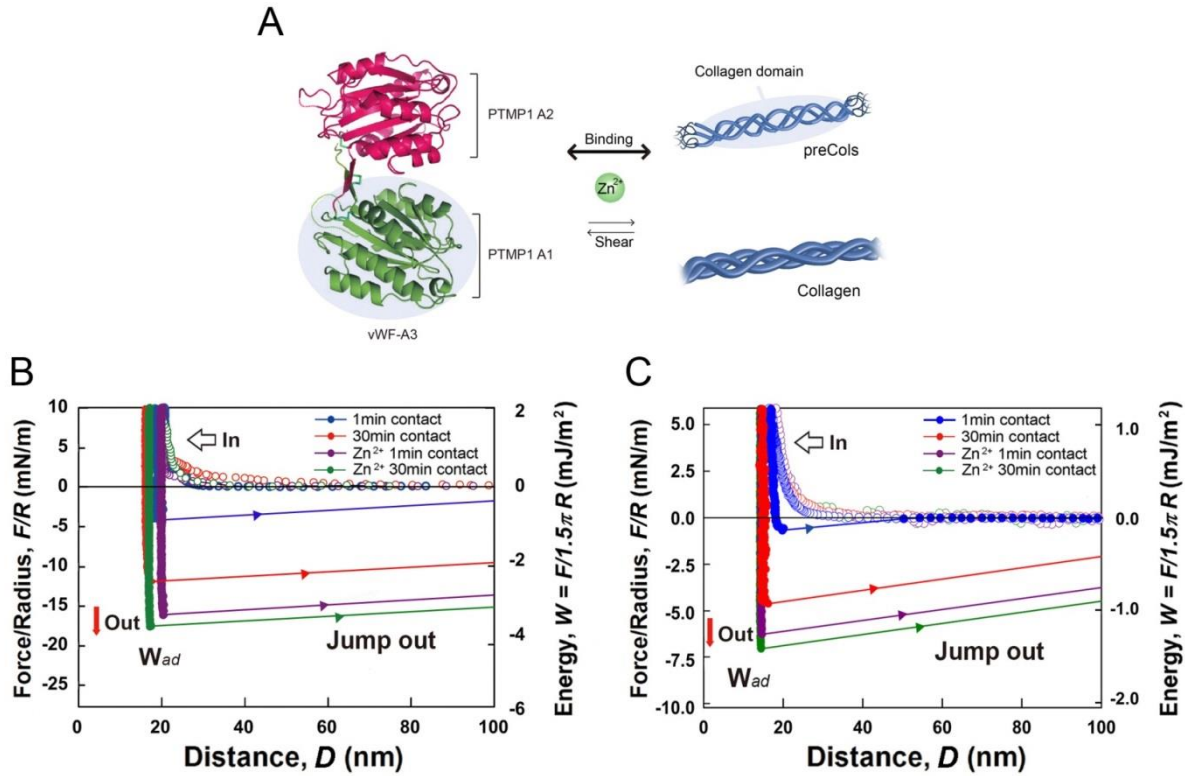
Figure 3. (A) Scheme of the PTMP1 structure showing the two vWF domains (PTMP1-A1 and PTMP1-A2). PTMP1-A1 (highlighted in blue) is similar to the I-domain of integrin a1. Binding of PTMP1 to preCols, which consist mainly collagen and Collagen Type I are investigated under addition of Zn^{2+} and Shearing effect. (B) PTMP1 adhesion to preCols in buffer condition pH 8.0 and injection of Zn^{2+}, (C) PTMP1 adhesion to collagen in buffer condition pH 8.0 and Zn^{2+} injection. The normalized forces, F/R is denoted in the left ordinate, whereas the corresponding interaction energies per unit area, W (defined by $W = F/1.5\pi R$) is on the right ordinate. W_{ad} is the adhesion energy per unit area ($W_{ad} = F_{ad}/1.5\pi R$). Open circle shows "in" (approach) and filled circle is "out" (separation).
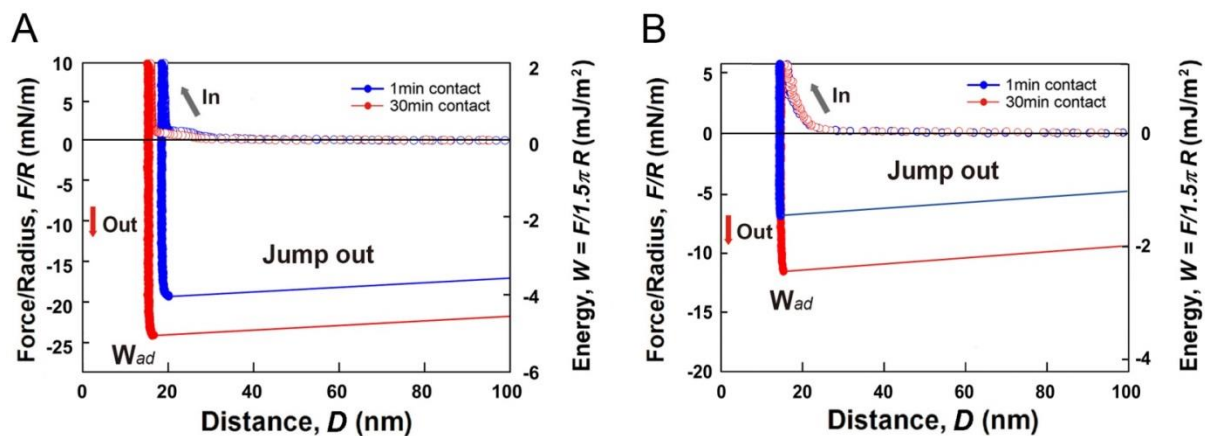
Figure 4. SFA studies of PTMP1 adhesion to preCols or collagen after shear in buffer condition pH 8.0: (A) PTMP1 and preCols interaction, and (B) PTMP1 and Collagen. The normalized forces, *F/R* is denoted in the left ordinate, whereas the corresponding interaction energies per unit area, *W* (defined by $W = F/1.5\pi R$) is on the right ordinate. W_{ad} is the adhesion energy per unit area ($W_{ad} = F_{ad}/1.5\pi R$). Open circle shows "in" (approach) and filled circle is "out" (separation).
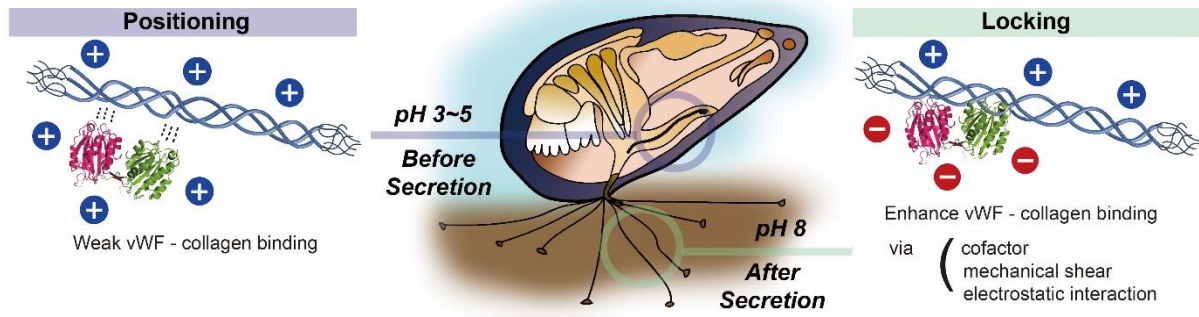
Figure 5. Adhesion mechanisms of PTMP1 and preCols in the secretion gland and after forming the byssal thread.